Solvation in high-temperature electrolyte solutions. III. Integral equation calculations and interpretation of experimental data

A. A. Chialvo[a)]
High Temperature Aqueous Chemistry Group, Chemistry and Analytical Sciences Division, Oak Ridge National Laboratory, Oak Ridge, Tennessee 37831-6110 and Department of Chemical Engineering, University of Tennessee, Knoxville, Tennessee 37996-2200

P. G. Kusalik
Department of Chemistry, Dalhousie University, Halifax, Nova Scotia, B3H 4J3, Canada

P. T. Cummings
Chemical Technology Division, Oak Ridge National Laboratory, Oak Ridge, Tennessee 37831-6268 and Departments of Chemical Engineering, Chemistry and Computer Science, University of Tennessee, Knoxville, Tennessee 37996-2200

J. M. Simonson
High Temperature Aqueous Chemistry Group, Chemical and Analytical Sciences Division, Oak Ridge National Laboratory, Oak Ridge, Tennessee 37831-6110

(Received 17 August 2000; accepted 4 December 2000)

The solvation of infinitely dilute aqueous Cl^-, Br^-, I^-, Cs^+, K^+, M^+, and the corresponding salts is analyzed by integral equation calculations along three near critical water isotherms according to the recently proposed molecular-based formalism which connects the solvent environment around individual ionic species with their macroscopic solvation behavior. Special emphasis is placed on the temperature dependence of some solvation-related macroscopic properties that are identified as potential candidates for the development of improved engineering correlations. Formal and integral equation calculations are then used to interpret recent experimental data, and some relevant theoretical implications regarding the modeling of high-temperature aqueous electrolyte solutions are discussed. © *2001 American Institute of Physics.* [DOI: 10.1063/1.1343875]

I. INTRODUCTION

Hydrothermal solution chemistry reveals a number of potential applications in a wide range of disciplines, including high-temperature microbiology,[1,2] hydrogen-rich fuel gas production from biomass,[3] synthesis of textured materials,[4–6] and oxidation of chemical and biochemical wastes.[7,8] With these applications come also new fundamental and technological challenges, such as metal corrosion,[9] clogging solid deposition on reactor pipes,[10,11] and catalysis of undesired reactions[12] by solvated ions.

Effort has been expended in the study of hydrothermal solutions to determine their thermodynamic, transport, and spectroscopic properties in order to meet these technological challenges in the design of effective processes.[13–15] A major objective behind this enterprise is to generate a fundamentally-based understanding of high-temperature solvation of species over a wide range of molecular asymmetries, including imperfect gases, ionic, polar, and nonpolar compounds.[16] Molecular asymmetry, the actual source of solution nonideality,[17] translates typically into pronounced gradients of solvent local density around charged species. In turn, these solvent inhomogeneities give rise to electrostriction and dielectric saturation phenomena, which render traditional solvation approaches inadequate.[18,19,20]

The failure of conventional solvation approaches for the description of hydrothermal solutions can be understood by recognizing that the formation of these solutions involved the coexistence of processes with disparate length scales, i.e., short-ranged (solvation) and long-ranged (compressibility-driven) phenomena.[21] In particular, the presence of compressibility-driven phenomena makes near-critical hydrothermal systems extremely challenging to model, unless we sort and isolate the (compressibility-driven) propagation of the density perturbation from the (solvation-related) finite-density perturbation phenomena.[22]

In this paper, part III of a series on ion solvation[23,24] we briefly review the main features of the molecular formalism for high-temperature electrolyte solutions recently proposed to tackle such a challenge[24] (Sec. II). Then, we illustrate the formalism by performing integral equation calculations of model aqueous electrolyte solutions for a variety of alkali metal halides (Sec. III), and use these results to interpret recent experimental data for aqueous alkali halide solutions[25] (Sec. IV). Finally, we discuss a molecular interpretation for the success of the recently proposed regression approach for the solute partial molar volumes,[25,26] and suggest a more appropriate alternative for the modeling of these systems.

II. HIGH-TEMPERATURE SOLVATION OF ELECTROLYTES

The solvation formalism that we have recently presented (part II of this series[24]) is based on the discrimination between the two length-scale phenomena associated with the formation of the solution, i.e., solvation and compressibility-

a)Author to whom correspondence should be addressed.

driven phenomena.[21,22] This is achieved by splitting the species total correlation functions into their direct and indirect contributions according to the Ornstein–Zernike (OZ) equation.[24]

The solvation of a salt $C^{\nu_+}A^{\nu_-}$ in a solvent at constant state conditions, where C^{ν_+} is the cation and A^{ν_-} is the anion, can be portrayed by the following *thought experiment* (see Fig. 1 of part II) on a system initially considered as a pure solvent in which ν solvent molecules ($\nu=\nu_+ + \nu_-$, where ν_+ and ν_- are the stoichiometric coefficients of the salt) are distinguishable by their *solute* labels. As such, this system constitutes an *ideal solution* in the sense of the Lewis–Randall Rule.[17,27] The *experiment* proceeds with the mutation of the distinguishable ν solvent molecules into the final neutral ionic solute $C^{\nu_+}A^{\nu_-}$ to form the infinitely dilute *nonideal solution*. This process in which the original ν *solute* species in the *ideal solution* (where solute–solvent interactions are identical to solute–solute and solvent–solvent interactions) are converted into the neutral ionic solute, is driven by the difference of free energy $[\mu_U^{r\infty}(T,P) - \nu\mu_V^{ro}(T,P)]$, where subscripts U and V denote solute and solvent species, respectively.

Our goal is the unambiguous characterization of the solvation process by drawing rigorous connections between the microscopic changes of the solvent structure around the mutating species and the relevant macroscopic (thermodynamic) properties. As we discussed elsewhere[28] there are at least four equivalent ways of interpreting the driving force of the solvation process, from either a microscopic or a macroscopic perspective. For the sake of brevity, and to support our forthcoming analysis and subsequent interpretation, here we describe a few relevant expressions, considering the neutral ionic solute as a hypothetical ''molecular'' entity in order to derive the solute properties that are usually measured experimentally. These results are then used for illustration purposes (for the individual ion counterpart the reader should consult part II) to interpret the most recent experimental data, and to suggest fundamentally-based alternatives for the regression of experimental raw data.

To display the four alternative interpretations we start from the exact thermodynamic expression for the driving force,

$$\mu_U^{r\infty}(T,P) - \nu\mu_V^{ro}(T,P) = \int_0^{\rho(P)} (\overline{v}_U^{\infty} - \nu\overline{v}_V^{o})\frac{d\rho}{\kappa\rho}, \tag{1}$$

where the superscript r denotes a residual quantity for a pure (o) or an infinitely dilute (∞) species at the indicated state conditions, respectively; T is the absolute temperature; P is the total pressure; $\overline{v}_V^{o}=v_V^{o}$ is the partial molar volume of the pure solvent such that $\rho=1/\overline{v}_V^{o}$ is its molar density counterpart; κ is the solvent isothermal compressibility; and $\overline{v}_U^{\infty}$ is the solute partial molar volume. We can now rewrite Eq. (1) in terms of the rate of change of pressure (at constant temperature and solvent density) caused by the structural perturbation of the solvent around the solute, i.e., $(\partial P/\partial x_U)_{T,\rho}^{\infty}$,[24]

$$\mu_U^{r\infty}(T,P) - \nu\mu_V^{ro}(T,P) = \int_0^{\rho(P)} \left(\frac{\partial P}{\partial x_U}\right)_{T,\rho}^{\infty} \frac{d\rho}{\rho^2}. \tag{2}$$

Equation (2) stresses that the integrand is finite at any state condition, and allows us to make contact with the microstructure of the system,[22] i.e. (see Appendix B of Chialvo *et al.*[24]),

$$\left(\frac{\partial P}{\partial x_U}\right)_{T,\rho}^{\infty} = \nu\rho kT(C_{VV}^{o} - C_{UV}^{\infty}), \tag{3}$$

where C_{VV}^{o} and C_{UV}^{∞} are the direct correlation function integrals (DCFI) for the solvent–solvent and solute–solvent interactions (i.e., the descriptors of the solution microstructure),[29,30] and k is the Boltzmann constant.

Another alternative expression for the driving force is obtained through the excess particle number,[22]

$$N_{U,\mathrm{ex}}^{\infty} = 4\pi\rho\int_0^{\infty}[g_{UV}^{\infty}(r) - g_{VV}^{o}(r)]r^2dr$$
$$= -\kappa(\partial P/\partial x_U)_{T,\rho}^{\infty} \tag{4}$$

that represents the number of solvent molecules around the solute in excess of that around any solvent molecule, i.e., around the solute in the Lewis–Randall ideal solution. Thus, after invoking its solvation contribution $N_{U,\mathrm{ex}}^{\infty}(\mathrm{SR}) = (\kappa^{IG}/\kappa)N_{U,\mathrm{ex}}^{\infty}$ (Ref. 28) we obtain

$$\left(\frac{\partial P}{\partial x_U}\right)_{T,\rho}^{\infty} = -\frac{N_{U,\mathrm{ex}}^{\infty}(\mathrm{SR})}{\kappa^{IG}}, \tag{5}$$

where $\kappa^{IG}=(\rho kT)^{-1}$ is the isothermal compressibility of the ideal gas at the state conditions of the solvent, and SR denotes a short-ranged contribution (associated with the local solvent density perturbation) to the corresponding diverging $N_{U,\mathrm{ex}}^{\infty}$. This equation emphasizes the explicit connection between the pressure perturbation (at constant T and ρ) associated with the disruption of the solvent structure around the solute and the corresponding effective change in the number of solvating (directly correlated to the solute) solvent molecules. Note that $N_{U,\mathrm{ex}}^{\infty}(\mathrm{SR})$ does not involve any assumption regarding the size of the solvation shell, as opposed to the conventional definition of coordination (or solvation) numbers which relies on an ambiguous choice of a radius based on some structural information of the solvation shell. In this sense, $N_{U,\mathrm{ex}}^{\infty}(\mathrm{SR})$ can be described as an *effective* solvation number (not to be confused with a coordination number[24,28]) since its knowledge allows us to reconstruct rigorously all other solvation properties.

Analogously, the pressure derivative $(\partial P/\partial x_U)_{T,\rho}^{\infty}$ can be rewritten in volumetric terms as[24]

$$\left(\frac{\partial P}{\partial x_U}\right)_{T,\rho}^{\infty} = kT\rho^2(\overline{v}_U^{\infty}(\mathrm{SR}) - \nu\overline{v}_V^{o}) \tag{6}$$

so that the difference of chemical potentials in Eq. (1) can be macroscopically interpreted not only in terms of the finite pressure perturbation $(\partial P/\partial x_U)_{T,\rho}^{\infty}$ as in Eq. (2), but also in terms of either the corresponding finite volumetric perturbation $(\overline{v}_U^{\infty}(\mathrm{SR}) - \nu\overline{v}_V^{o})$, or the resulting *effective* solvation number $N_{U,\mathrm{ex}}^{\infty}(\mathrm{SR})$ as follows:

$$\mu_U^{r\infty}(T,P)-\nu\mu_V^{ro}(T,P)=kT\int_0^{\rho(P)}(\overline{v}_U^{\infty}(\mathrm{SR})-\nu\overline{v}_V^{o})d\rho$$

$$=-kT\int_0^{\rho(P)}N_{U,\mathrm{ex}}^{\infty}(\mathrm{SR})\frac{d\rho}{\rho}. \quad (7)$$

As we have already discussed[24,28] the properties available from experiment are those of the hypothetical electroneutral ionic salt. However, the salt properties at infinite dilution are actually linear combinations of the corresponding single-ion counterparts, and therefore, the solvation quantities for salts can be expressed in terms of the corresponding pressure, solvation number or density perturbation around the individual ions (the actual species in solution). This will not be addressed here since it has been discussed in much detail elsewhere.[28]

In summary, in the preceding analysis we have given equivalent ways to express the finite change of free energy in the solvation process that creates an infinitely dilute *nonideal* mixture from the original *ideal solution*, when ν solvent molecules are *mutated* into ν_+ cations and ν_- anions in solution. The resulting solvation properties are well-behaved state-dependent quantities; the enthalpic and entropic contributions to the free energy change on solvation are discussed in detail elsewhere.[21,24] Yet, their temperature and pressure derivatives will diverge at the solvent criticality,[31] a behavior that implies an advantageous (and not always well appreciated) exact cancellation between the corresponding divergent portions of the enthalpic and entropic contributions to $(\mu_U^{r\infty}(T,P)-\nu\mu_V^{ro}(T,P))$. These diverging contributions to the partial molar enthalpy and entropy of the solute at infinite dilution are not associated with the solvation process (the local perturbation) but rather with the propagation of the perturbation across the system, and are characterized by the correlation length of the solvent. This feature suggests the need for a precise sorting between the two contributions, i.e., separating solvation from compressibility-driven phenomena, to avoid working with unnecessary implicitly diverging quantities in the modeling of dilute solutions in highly-compressible media. Note that O'Connell and colleagues[30,32–34] have developed macroscopic models, based on the regression of experimental data to determine the direct correlation function integrals as functions of state conditions and composition, and subsequently, to calculate the thermodynamic properties of a variety of systems according to the Kirkwood–Buff fluctuation theory of solutions.[35]

III. INTEGRAL EQUATION CALCULATIONS AND INTERPRETATION OF EXPERIMENTAL RESULTS

A. Models, methodology, and state conditions

In this section we study the solvation behavior of a variety of anions and cations, covering a wide range of ionic diameters $1.08<d_i/d_V<1.96$ (where d_i and d_V denote the diameters of the individual ions and the solvent, respectively) along three near-critical isotherms (643 K, 673 K, and 703 K), in the density range $0.0136\leqslant\rho(\mathrm{g/cm^3})\leqslant 0.81$. In the present calculations the systems are defined as charged hard sphere ions immersed in a model aqueouslike solvent, represented by hard spheres with embedded point polarizabilities and permanent electrostatic multipole moments including quadrupole and octupoles as given in Tables I and II. The calculations were carried out by solving the reference hypernetted-chain (RHNC) equations with solvent polarization effects treated at the self-consistent mean-field (SCMF) level as described elsewhere.[36,37] Details on these calculations for systems at normal conditions were presented earlier,[38,39] and some others for high temperature solutions are given elsewhere.[24,28] In addition, and in contrast to the normal unit charges, the ions bear only a 66% of the full charge. The reduced charges were necessary to avoid the collapse of solvent molecules on bare ions thus ensuring the convergence of the integral equation calculations over the entire solvent density range considered.[24,28]

TABLE I. Molecular properties of the waterlike solvent (V).

Property	Value
d_ν	2.8 Å
μ	1.85×10^{-18} esu cm
α_{xx}	1.501 Å^3
α_{yy}	1.390 Å^3
α_{zz}	1.442 Å^3
Q_{xx}	2.63×10^{-26} esu cm^2
Q_{yy}	-2.50×10^{-26} esu cm^2
Q_{zz}	-0.13×10^{-26} esu cm^2
Ω_{xxz}	2.30×10^{-34} esu cm^3
Ω_{yyz}	-0.96×10^{-34} esu cm^3
Ω_{zzz}	-1.34×10^{-34} esu cm^3

In order to make a meaningful comparison between model predictions and experimental results, we first estimated the solvent critical conditions based on the divergence of the isothermal compressibility. According to the predicted isothermal density dependence of the isothermal compressibility, Fig. 1, the critical point of this waterlike solvent is $T_c\leqslant 643$ K and $\rho_c\approx 0.20$ g/cm^3, i.e., the three isotherms considered in this study are supercritical. The corresponding $P-\rho-T$ behavior of the model solvent along the isotherms 643 K, 673 K, and 703 K is presented in Fig. 2.

B. Integral equation results

We targeted the solvent properties including the dipole moment, the dielectric constant, the pressure, the isothermal compressibility, and the ion partial molar volumes at infinite dilution.[36–38] Based on these properties, and according to the solvation formalism, we determined the properties of the nine resulting salts (U) at infinite dilution, i.e., CsBr, CsCl, CsI, KBr, KCl, KI, MBr, MCl, and MI, where M^+ might

TABLE II. Reduced ion diameter $d_i^*=d_i/d_V$ used in this work.

Ion	d_i^*
K^+	1.08
Cl^-	1.16
Cs^+	1.28
Br^-	1.28
I^-	1.44
M^+	1.96

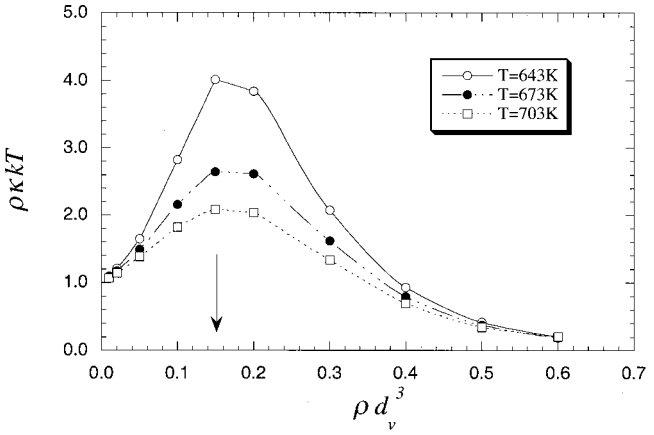

FIG. 1. Isothermal density dependence of $\rho kT\kappa$ for the pure waterlike solvent according to the RNHC calculations. The arrow indicates the estimated critical density.

represent an alkylammonium cation.[39] In particular, we focus our attention on the isothermal density-dependence of $\overline{v}_U^{\infty}$, $\overline{v}_U^{\infty}(\mathrm{SR})$, $(\partial P/\partial x_U)_{T,\rho}^{\infty}$, $N_{U,\mathrm{ex}}^{\infty}(\mathrm{SR})$, and some related microscopic analogs.[24]

1. Salt partial molar volumes and their solvation counterparts

In Figs. 3(a)–11(a) we display the isothermal density dependence of the salt partial molar volumes along the three supercritical isotherms. As we might have expected, based on the strength of the ion–water interactions relative to that for the water–water interactions, these partial molar properties are negative and eventually diverge to minus infinity as the solvent approaches its critical point. In the classification scheme used in the supercritical fluid community, these salts behave as attractive[40] or nonvolatile[41] solutes, i.e., because the ion–water interactions are stronger than the water–water interactions, the volumetric perturbation in the process of inserting the ions in water during the solvation process translates into a volume contraction (see below the pressure and solvation number counterparts). Obviously, for this type of solute–solvent model, the volumetric perturbation on the solvent structure becomes larger with decreasing ion sizes or increasing ion charge density.

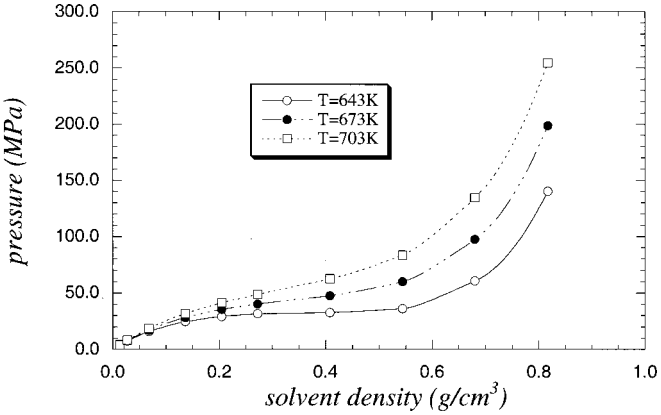

FIG. 2. Isothermal density dependence of the total pressure for the pure waterlike solvent according to the RHNC calculations.

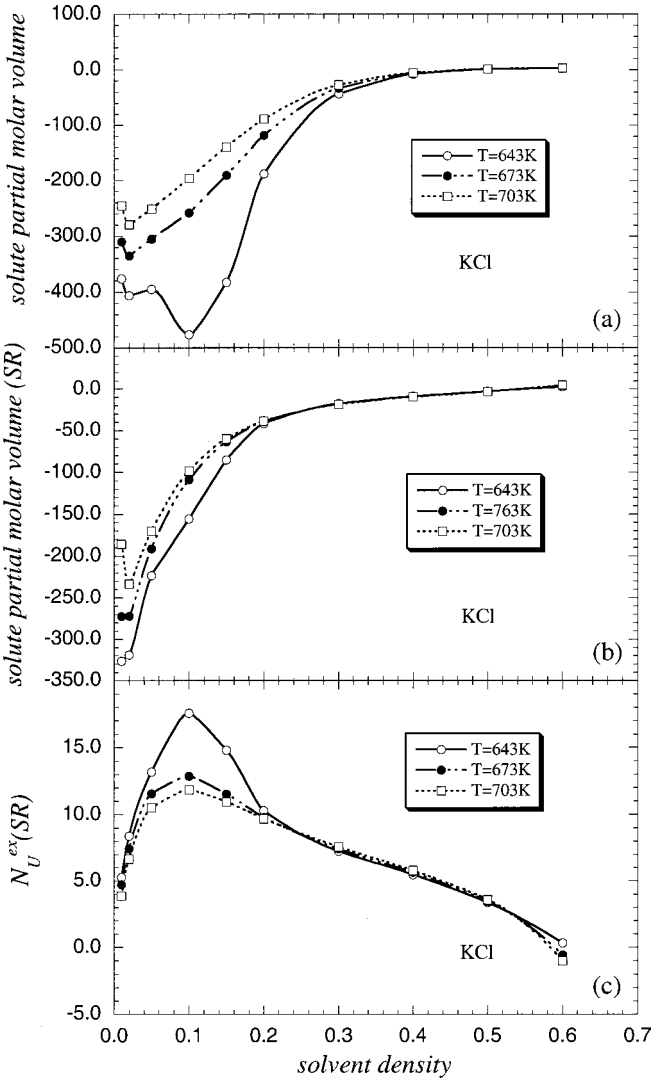

FIG. 3. Isothermal density dependence of (a) $\overline{v}_U^{\infty}$, (b) $\overline{v}_U^{\infty}(\mathrm{SR})$, and (c) $N_{U,\mathrm{ex}}^{\infty}(\mathrm{SR})$ for an infinitely dilute KCl aqueous solution. Volumes and densities in units of d_V^3.

In all cases the partial molar volume exhibits a minimum at a density smaller than the solvent's critical density. This minimum shifts to smaller densities as the temperature increases. The magnitude of $\overline{v}_U^{\infty}$ at this minimum is approximately inversely proportional to the *diameter* d_U given by $d_U = d_+ + d_-$, i.e., $d_{\mathrm{MI}} > d_{\mathrm{MBr}} > d_{\mathrm{MCl}} > d_{\mathrm{CsI}} > d_{\mathrm{CsBr}} > d_{\mathrm{KI}} > d_{\mathrm{CsCl}} > d_{\mathrm{KBr}} > d_{\mathrm{KCl}}$. Moreover, the partial molar volume increases with solvent density and eventually becomes positive for densities twice the critical value. The trend of the density dependence of $\overline{v}_U^{\infty}$ at the crossover indicates that the larger the salt the more positive the resulting partial molar volumes. This behavior suggests that even attractive (nonvolatile) solutes at near-critical densities, such as strong electrolytes in aqueous solution, might become repulsive solutes in denser environments (see below the corresponding pressure and solvation number perturbation counterparts).

Note also that the partial molar volumes at supercritical

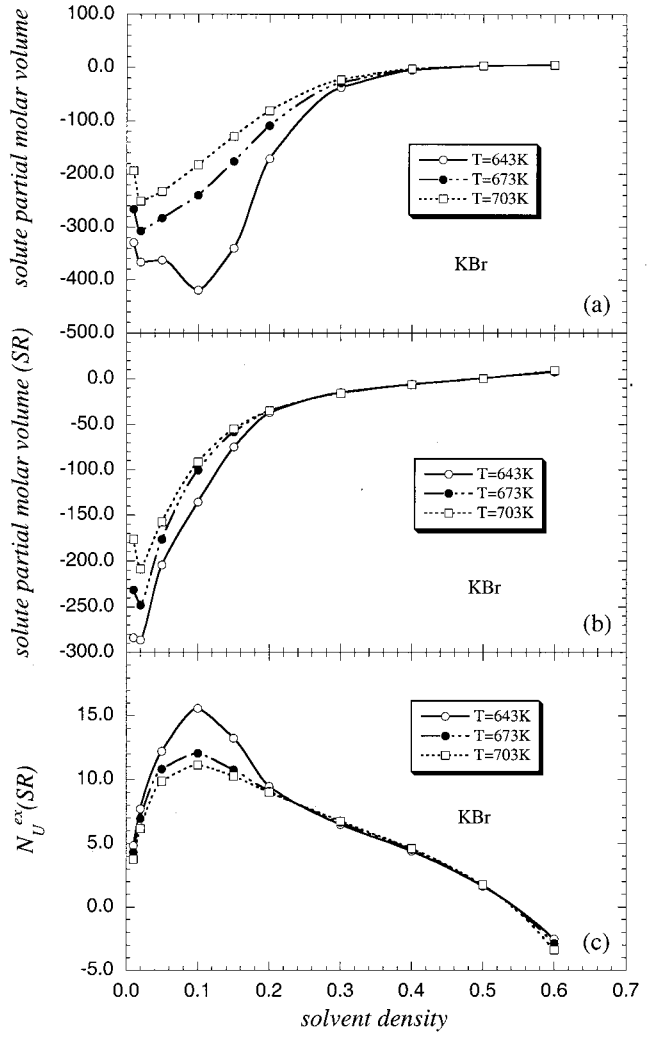

FIG. 4. Isothermal density dependence of (a) $\overline{v}_U^{\infty}$, (b) $\overline{v}_U^{\infty}$(SR), and (c) $N_{U,\mathrm{ex}}^{\infty}$(SR) for an infinitely dilute KBr aqueous solution. Volumes and densities in units of d_V^3.

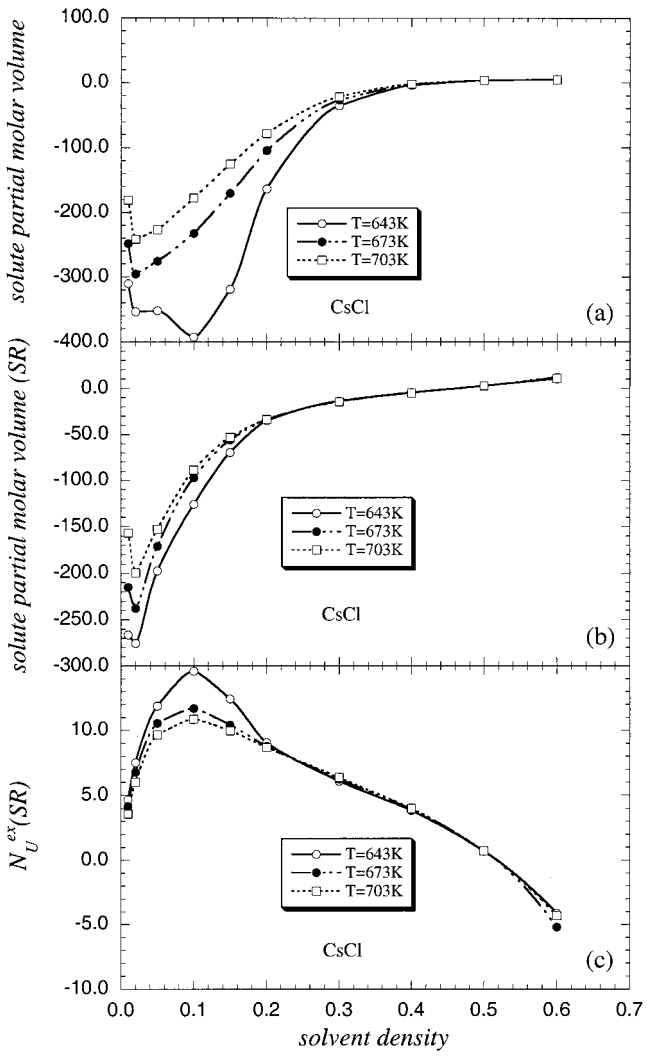

FIG. 5. Isothermal density dependence of (a) $\overline{v}_U^{\infty}$, (b) $\overline{v}_U^{\infty}$(SR), and (c) $N_{U,\mathrm{ex}}^{\infty}$(SR) for an infinitely dilute CsCl aqueous solution. Volumes and densities in units of d_V^3.

densities exhibit a negligibly small temperature dependence, a behavior that will take center stage in the next section. In fact, the temperature independence of $\overline{v}_U^{\infty}$ is noted over a wide supercritical density range [in this study $\rho d_V^3 \geqslant \rho_c d_V^3$, see Figs. 3(b)–11(b)]. Note that, in contrast to the behavior of the full partial molar volume $\overline{v}_U^{\infty}$, the solvation contribution $\overline{v}_U^{\infty}$(SR) displays a clear minimum around $\rho d_V^3 \approx 0.02$, a density that appears to be independent of either temperature or type of solute. At this minimum, the magnitude of $\overline{v}_U^{\infty}$(SR) follows the same trend with d_U as $\overline{v}_U^{\infty}$, i.e., the smaller the salt size, the larger is the solvation contribution to the salt partial molar volume.

2. Solvation numbers

In Figs. 3(c)–11(c) we present the isothermal density dependence of the solvation number $N_{U,\mathrm{ex}}^{\infty}$(SR) in comparison with the corresponding $\overline{v}_U^{\infty}$(SR). Because of the direct connection between the two quantities [see Eqs. (5) and (6)],

$$N_{U,\mathrm{ex}}^{\infty}(\mathrm{SR}) = \nu - \rho \overline{v}_U^{\infty}(\mathrm{SR}), \tag{8}$$

this quantity exhibits many of the same features as the corresponding $\overline{v}_U^{\infty}$(SR), in particular, the lack of temperature dependence for supercritical densities, and a maximum value around $\rho d_V^3 \approx 0.1$ which also appears to be independent of either the temperature or the type of ions.

At subcritical densities, the solvation numbers $N_{U,\mathrm{ex}}^{\infty}$(SR) are positive, reflecting the condition of attractive (nonvolatile) solutes. At the maximum ($\rho d_V^3 \approx 0.1$) these solvation numbers range from ~18 for KCl to ~8 for MI. Moreover, as the solvent density increases, these solvation numbers decrease toward negative values, i.e., the solutes become repulsive (volatile) species. This crossover occurs around $\rho d_V^3 \geqslant 0.6$ for KCl, and moves to smaller densities with increasing ion size, i.e., to $\rho d_V^3 \approx 0.3$ for MI. Consequently, while KCl behaves as an attractive solute over essentially the entire range of densities studied here ($0 < \rho < 3.3\rho_c$), the remaining eight solutes change their behavior from attractive to repulsive species, as indicated by the negative solvation numbers at $\rho d_V^3 = 0.6$ which vary from $N_{U,\mathrm{ex}}^{\infty}(\mathrm{SR}) \approx -3$ for KBr to $N_{U,\mathrm{ex}}^{\infty}(\mathrm{SR}) \approx -34$ for MI.

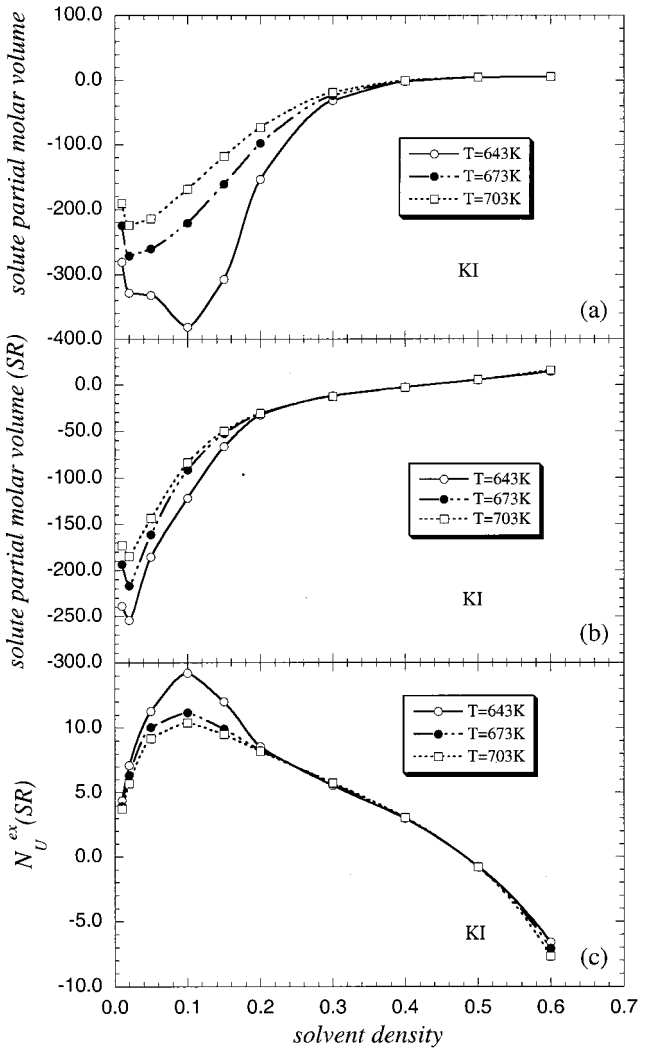

FIG. 6. Isothermal density dependence of (a) $\overline{v}_U^{\infty}$, (b) $\overline{v}_U^{\infty}$(SR), and (c) $N_{U,\mathrm{ex}}^{\infty}$(SR) for an infinitely dilute KI aqueous solution. Volumes and densities in units of d_V^3.

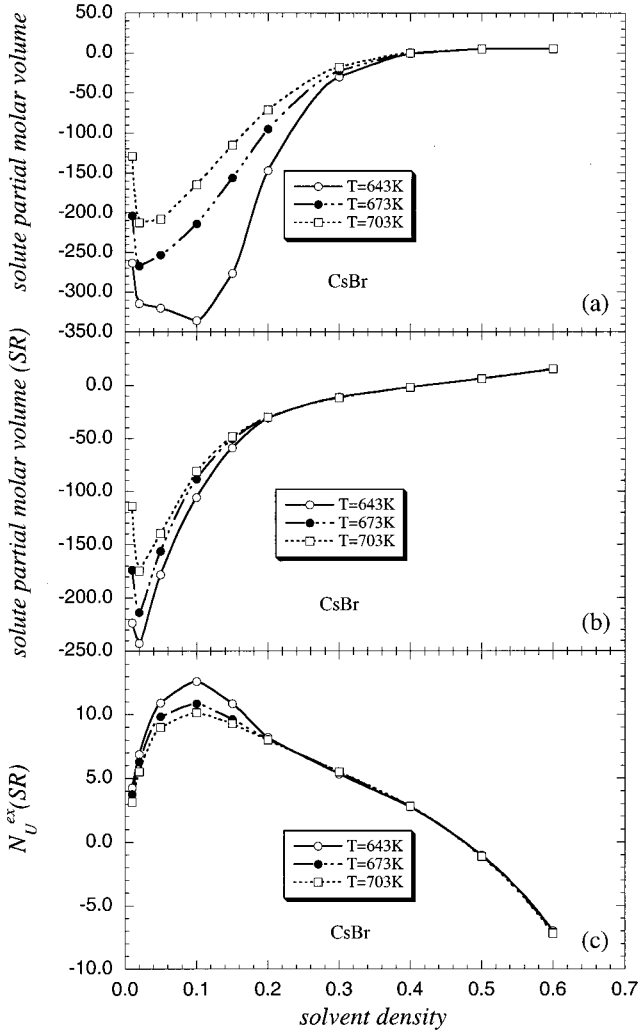

FIG. 7. Isothermal density dependence of (a) $\overline{v}_U^{\infty}$, (b) $\overline{v}_U^{\infty}$(SR), and (c) $N_{U,\mathrm{ex}}^{\infty}$(SR) for an infinitely dilute CsBr aqueous solution. Volumes and densities in units of d_V^3.

3. Salt pressure perturbation parameter

In Figs. 12–14 we present the isothermal density dependence of the pressure perturbation $(\partial P/\partial x_U)_{T,\rho}^{\infty}$. Because of its direct connection to the solvation number [see Eq. (5)], there is only a weak change on the density and temperature dependence of $(\partial P/\partial x_U)_{T,\rho}^{\infty}$ with respect to that of $N_{U,\mathrm{ex}}^{\infty}$(SR), resulting from the explicit proportionality with $\kappa^{IG}=1/\rho kT$. The pressure perturbation $(\partial P/\partial x_U)_{T,\rho}^{\infty}$ becomes negative and exhibits a rather flat minimum at a supercritical density, consistent with the attractive (nonvolatile) nature of the salt. However, and as already observed in the associated solvation properties, $(\partial P/\partial x_U)_{T,\rho}^{\infty}$ becomes positive with increasing density, i.e., the salts change from attractive to repulsive solutes. Obviously, this change of behavior for the neutral salt depends on the magnitude and sign of the quantities for the individual ions, since $(\partial P/\partial x_U)_{T,\rho}^{\infty}=\nu_-(\partial P/\partial x_-)_{T,\rho}^{\infty}+\nu_+(\partial P/\partial x_+)_{T,\rho}^{\infty}$ [see Eq. (39) in part II]. All ions in this study display the same attractive-to-repulsive transition with isothermal increases in density (not shown explicitly in this paper), however, it is possible that a larger ion (than either I^- or M^+) might exhibit a repulsive behavior in the entire range of densities at supercritical temperatures. Likewise, it is also possible to find smaller (than K^+ or Cl^-) ions such that their stronger ion–solvent interactions will translate into attractive ions (salt) in the entire range of solvent densities.

C. Integral equation results vs experimental data

The main challenge for an experimentalist, beyond the arduous task of performing accurate measurements, is the proper interpretation of the raw data. This is obviously not an easy task, especially when dealing with potentially divergent quantities such as the observed partial molar properties of infinitely dilute solutes. In this section we would like to illustrate how the formalism described in Sec. II, in conjunction with integral equation calculations on model systems, can facilitate the interpretation of high-temperature solvation, and guide the selection of quantities to be used in the development of engineering correlations. For example, in a series of recent publications, Wood and co-workers[25,26] reported the most accurate values of partial molar properties

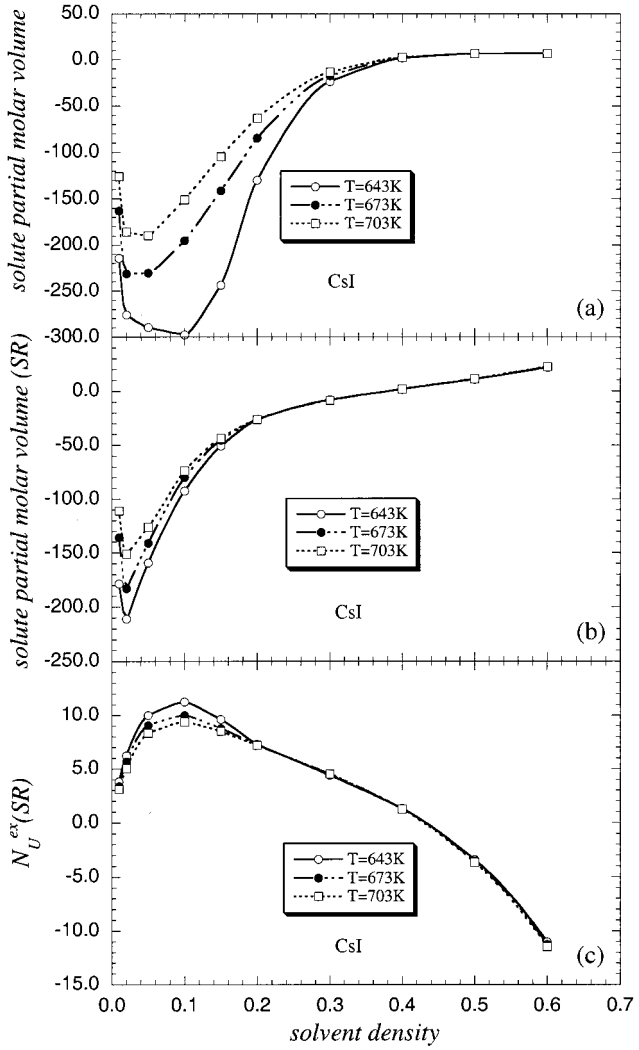

FIG. 8. Isothermal density dependence of (a) $\overline{v}_U^{\infty}$, (b) $\overline{v}_U^{\infty}$(SR), and (c) $N_{U,\mathrm{ex}}^{\infty}$(SR) for an infinitely dilute CsI aqueous solution. Volumes and densities in units of d_V^3.

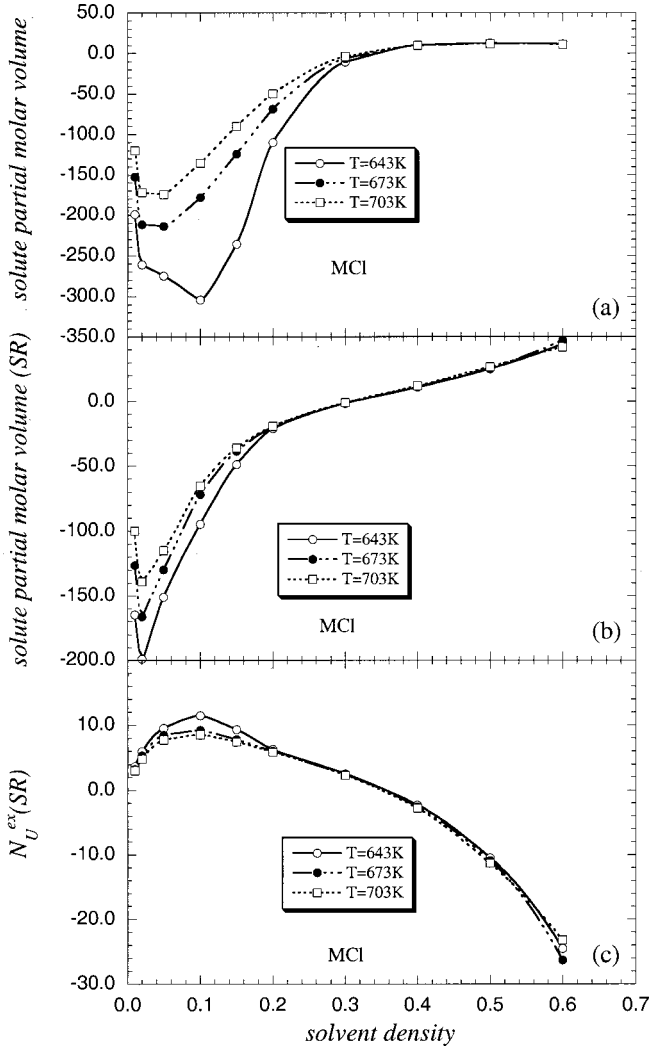

FIG. 9. Isothermal density dependence of (a) $\overline{v}_U^{\infty}$, (b) $\overline{v}_U^{\infty}$(SR), and (c) $N_{U,\mathrm{ex}}^{\infty}$(SR) for an infinitely dilute MCl aqueous solution. Volumes and densities in units of d_V^3.

for a series of ionic and nonionic species at infinite dilution in high-temperature aqueous solutions. They proposed a successful regression of the raw data in terms of the quantity $D_{UV}^{\infty}=(\kappa^{IG}/\kappa)\overline{v}_U^{\infty}$. This quantity exhibits an appealing weak temperature dependence in the range $550<T(\mathrm{K})<725$, which allows a rather simple and well-behaved density correlation to predict (in principle) $\overline{v}_U^{\infty}$ at any other supercritical state condition,[26] based solely on the thermodynamic properties of pure water. While the choice of properties involved in the quantity D_{UV}^{∞} was not accidental,[42] in that it contains all the components to cancel the potential divergence in $\overline{v}_U^{\infty}$, it is not clear why D_{UV}^{∞} should be more advantageous than other choices, or why the temperature dependence should be negligible.

In Fig. 15 we show the solvent density-dependence of D_{UV}^{∞} along three supercritical isotherms for infinitely dilute CsCl aqueouslike solutions as predicted by the integral equation calculations (A similar comparison has already been presented for CsBr in Ref. 28). We also compare these results with the corresponding data of Sedlbauer *et al.*,[25] which were determined from measurements yielding solute partial molar volumes at infinite dilution within the temperature and density ranges $604<T(\mathrm{K})<717$ and $0.26<\rho(\mathrm{g/cm^3})<0.60$, respectively. To be more precise, Sedlbauer *et al.* determined $\overline{v}_U^{\infty}$, and subsequently developed a simple density correlation of D_{UV}^{∞}, for NaCl, LiCl, NaBr, and CsBr. Based on this correlation, and considering that $\overline{v}_U^{\infty}=\nu_-\overline{v}_-^{\infty}+\nu_+\overline{v}_+^{\infty}$, we were able to estimate $D_{UV}^{\infty}(\mathrm{CsCl})=D_{UV}^{\infty}(\mathrm{CsBr})-D_{UV}^{\infty}(\mathrm{NaBr})+D_{UV}^{\infty}(\mathrm{NaCl})$ as indicated in the Appendix. Subsequently, we determined $(\partial P/\partial x_U)_{T,\rho}^{\infty}$ and $N_{U,\mathrm{ex}}^{\infty}$(SR) (Figs. 16 and 17) according to the calculated D_{UV}^{∞}(CsCl) and the corresponding properties of pure water.

The comparison displayed in Figs. 15–17 is only intended to show that the chosen intermolecular potential model is capable of predicting the same trends and magnitude of the solvation quantities of interest, i.e., by capturing the relevant physics underlying the solvation process.

IV. DISCUSSION AND FINAL REMARKS

We have characterized the solvation behavior of aqueous electrolytes and illustrated it with nine salts in high-temperature solutions through integral equation calculations

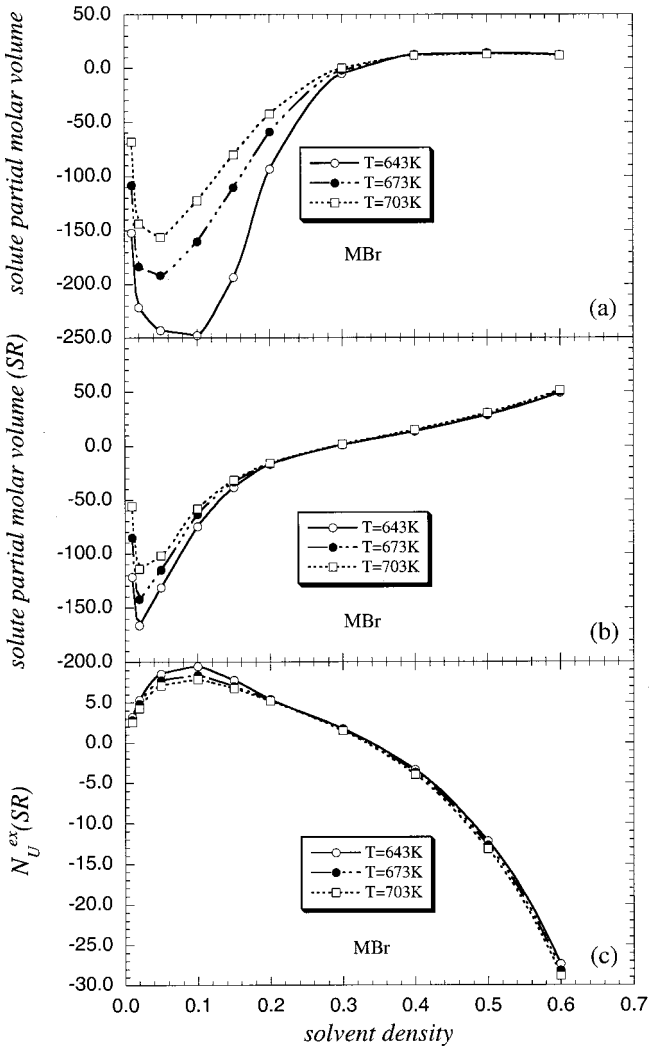

FIG. 10. Isothermal density dependence of (a) $\overline{v}_U^{\infty}$, (b) $\overline{v}_U^{\infty}(\mathrm{SR})$, and (c) $N_{U,\mathrm{ex}}^{\infty}(\mathrm{SR})$ for an infinitely dilute MBr aqueous solution. Volumes and densities in units of d_V^3.

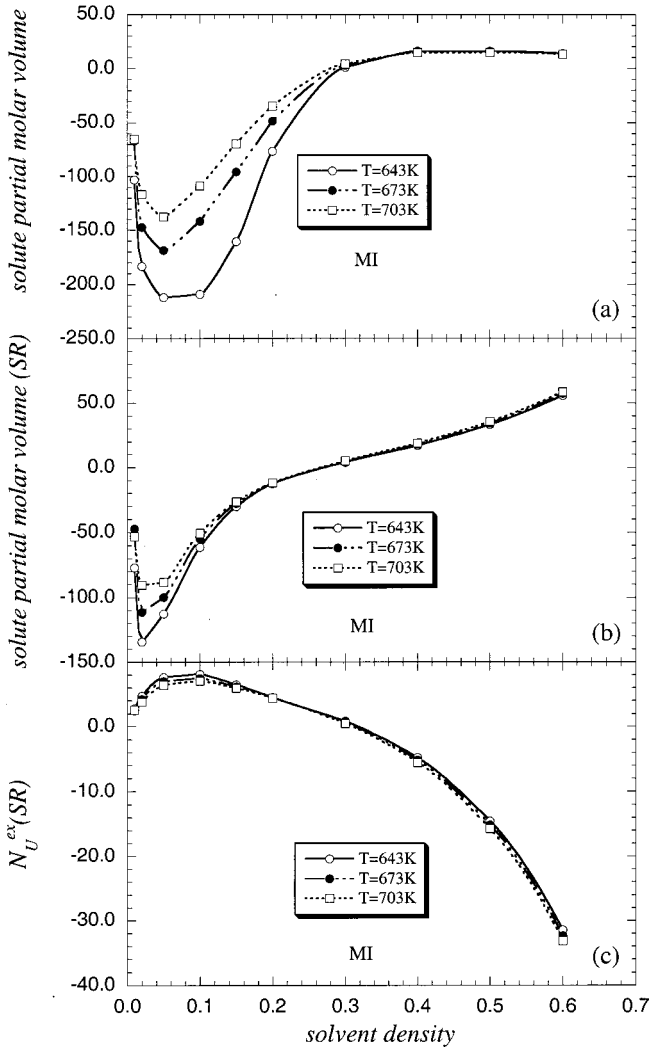

FIG. 11. Isothermal density dependence of (a) $\overline{v}_U^{\infty}$, (b) $\overline{v}_U^{\infty}(\mathrm{SR})$, and (c) $N_{U,\mathrm{ex}}^{\infty}(\mathrm{SR})$ for an infinitely dilute MI aqueous solution. Volumes and densities in units of d_V^3.

of simple (nonprimitive) aqueous electrolyte models, according to thermodynamic and statistical mechanical views. The task was achieved by determining the individual properties of six infinitely dilute ions in a waterlike solvent, and through discrimination between the true solvation phenomena and the largely unrelated accompanying compressibility-driven phenomena. These solvation-related properties have unambiguous microscopic meaning and can be determined experimentally from the isothermal compressibility of the pure solvent κ and the infinite-dilution partial molar properties.[24] For the case under consideration we have that the solvation contribution to $\overline{v}_U^{\infty}$ is given by,

$$\overline{v}_U^{\infty}(\mathrm{SR}) = (\kappa^{IG}/\kappa)(\overline{v}_U^{\infty} - \nu v_V^o) + \nu v_V^o, \tag{9}$$

where $\overline{v}_U^{\infty} = \nu_- \overline{v}_-^{\infty} + \nu_+ \overline{v}_+^{\infty}$; the solvation number,[43]

$$N_{U,\mathrm{ex}}^{\infty}(\mathrm{SR}) = (\kappa^{IG}/\kappa)(\nu - (\overline{v}_U^{\infty}/v_V^o)), \tag{10}$$

and the pressure perturbation,

$$\left(\frac{\partial P}{\partial x_U}\right)_{T,\rho}^{\infty} = (\overline{v}_U^{\infty}/v_V^o) - \nu)/\kappa. \tag{11}$$

Once again it is important to bear in mind that the excess number (or solvation number) $N_{U,\mathrm{ex}}^{\infty}(\mathrm{SR})$ and its ion counterparts should not be confused with the usual coordination number, described in terms of the geometric arrangement of solvent molecules around a central species.[44] Consequently, they cannot be compared with the conventional solvation/hydration numbers obtained through NMR, EXAFS, neutron or x-ray diffraction measurements.[45,46] The reason is rather obvious, on the one hand $N_{U,\mathrm{ex}}^{\infty}(\mathrm{SR})$ accounts for the solvent molecules *directly correlated* with the central species in excess over that for the (Lewis–Randall) ideal solution counterpart, and encompasses unambiguous connections with all solvation properties.[24] On the other hand, the conventional definition considers the solute–solvent coordination within an ambiguously defined solvation shell. Beyond the obvious ambiguity in the choice of the radius of solvation, which translates into solvation numbers that depend on the method of determination, there is no clear connection between these numbers and the relevant solvation properties. The rigorous connection between structure and macroscopic properties is given by statistical mechanical expressions involving either

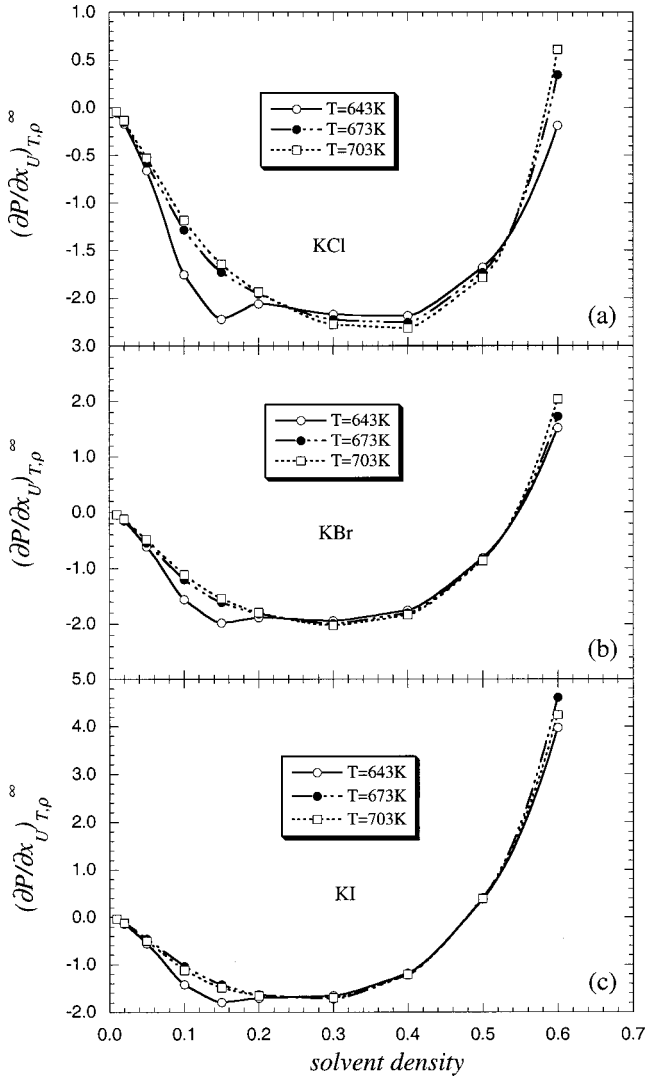

FIG. 12. Isothermal density dependence of $(\partial P/\partial x_U)^{\infty}_{T,\rho}$ for an infinitely dilute of (a) KCl, (b) KBr, and (c) KI aqueous solutions. Pressure in units of kT and d_V^3.

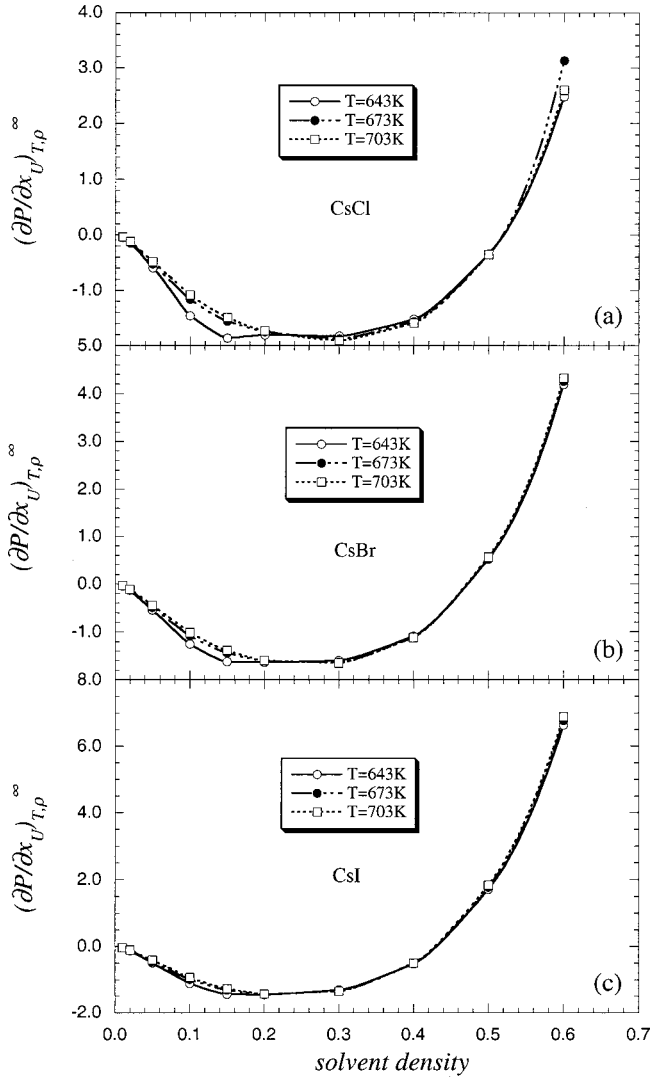

FIG. 13. Isothermal density dependence of $(\partial P/\partial x_U)^{\infty}_{T,\rho}$ for an infinitely dilute of (a) CsCl, (b) CsBr, and (c) CsI aqueous solutions. Pressure in units of kT and d_V^3.

the total or the direct correlation function integrals over the entire volume of the system. Therefore, the use of a portion of the total correlation function, that inside the solvation shell to define the coordination number, cannot account for the remaining contributions to properties beyond the solvation radius and requires the introduction of assumptions that render the resulting approach unreliable. In summary, knowledge of $N^{\infty}_{U,\mathrm{ex}}(\mathrm{SR})$ allows us to determine (rigorously) all solvation properties for the system under study, while the more familiar concept of solvation/hydration numbers does not.

Considering that one of the primary goals of our molecular-based studies is to provide the fundamental understanding needed to develop successful engineering correlations, we use the proposed solvation formalism as a powerful tool to interpret recent experimental data, and hopefully, to guide the choice of the best combination of properties for regression purposes. For example, the pronounced lack of temperature dependence of the predicted values of D^{∞}_{UV} for supercritical densities is an appealing behavior for regression purposes, and suggests some relevant questions regarding either the underlying microscopic mechanism or possible connections between D^{∞}_{UV} and well-defined solvation quantities. Since we have recently partially addressed the first item, here we will tackle the second one, through the interpretation of D^{∞}_{UV} in terms of the solvation quantities $N^{\infty}_{U,\mathrm{ex}}(\mathrm{SR})$, $(\partial P/\partial x_U)^{\infty}_{T,\rho}$, $\overline{v}^{\infty}_U(\mathrm{SR})$, and $\overline{v}^{\theta}_V(C^{\infty}_{UV}-C^{o}_{VV})$ by invoking Eqs. (3), (5), (6), and (8), i.e.,

$$\begin{aligned} D^{\infty}_{UV} &= D^{o}_{VV}+\nu\overline{v}^{o}_V(C^{o}_{VV}-C^{\infty}_{UV}) \\ &= D^{o}_{VV}-\overline{v}^{o}_V N^{\infty}_{U,\mathrm{ex}}(\mathrm{SR}) \\ &= D^{o}_{VV}+\overline{v}^{o}_V\kappa^{IG}\left(\frac{\partial P}{\partial x_U}\right)^{\infty}_{T,\rho} \\ &= D^{o}_{VV}-\nu\overline{v}^{o}_V+\overline{v}^{\infty}_U(\mathrm{SR}), \end{aligned} \tag{12}$$

where for convenience we define $D^{o}_{VV}\equiv\overline{v}^{o}_V(\kappa^{IG}/\kappa)=D^{\infty(IS)}_{UV}$ which is a property of the pure solvent, i.e., the ideal solution counterpart of D^{∞}_{UV}. Therefore, according to the above

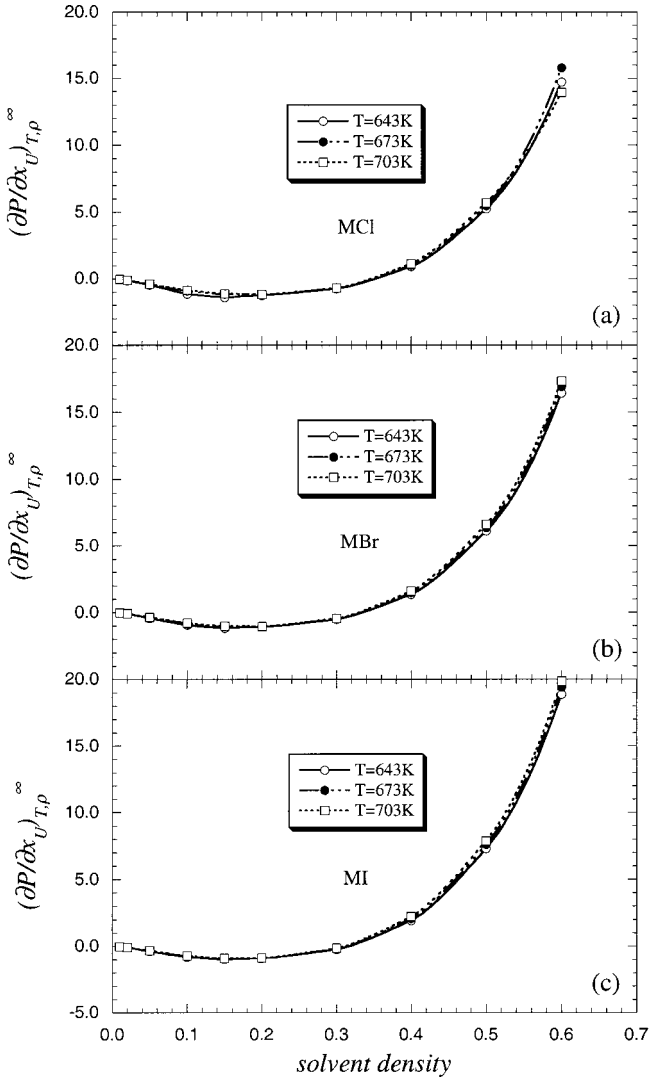

FIG. 14. Isothermal density dependence of $(\partial P/\partial x_U)^{\infty}_{T,\rho}$ for an infinitely dilute of (a) MCl, (b) MBr, and (c) MI aqueous solutions. Pressure in units of kT and d_V^3.

expressions and the observed behavior for the density dependence of the solvation quantities, a more appropriate regression quantity (than D^{∞}_{UV}) would be $\Delta D^{\infty}_{UV}=D^{\infty}_{UV}-\nu D^{\infty(IS)}_{UV}$, i.e.,

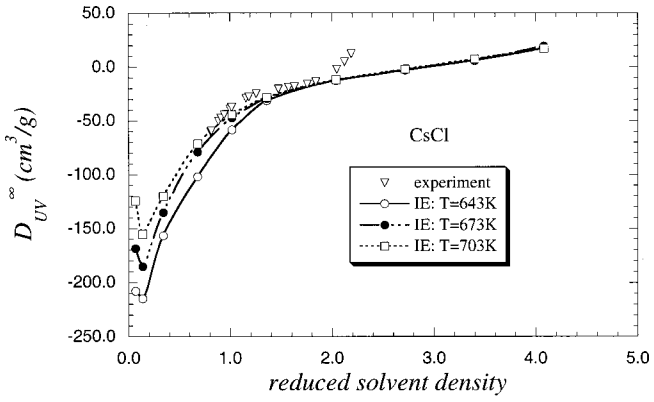

FIG. 15. Density dependence of D^{∞}_{UV} for CsCl aqueous solutions. Comparison between RHNC calculations and experimental data.

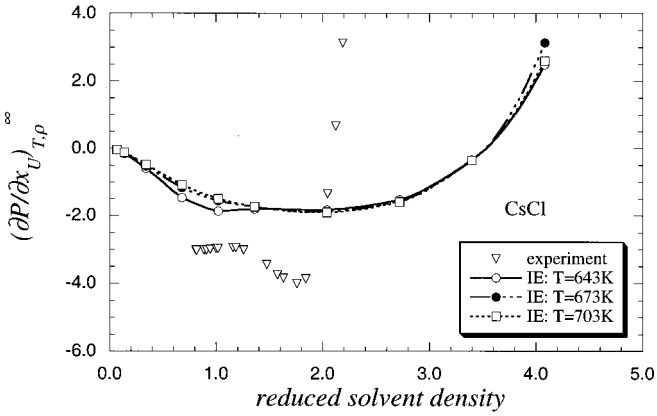

FIG. 16. Density dependence of $(\partial P/\partial x_U)^{\infty}_{T,\rho}$ for CsCl aqueous solutions. Comparison between RHNC calculations and experimental data. Pressure in units of kT and d_V^3.

$$\begin{aligned}\Delta D^{\infty}_{UV} &= \nu\overline{v}^{o}_{V}(C^{o}_{VV}-C^{\infty}_{UV})\\ &= -\overline{v}^{o}_{V}N^{\infty}_{U,\mathrm{ex}}(\mathrm{SR})\\ &= \overline{v}^{o}_{V}\kappa^{IG}\left(\frac{\partial P}{\partial x_U}\right)^{\infty}_{T,\rho}\\ &= \overline{v}^{\infty}_{U}(\mathrm{SR})-\nu\overline{v}^{o}_{V}\end{aligned} \tag{13}$$

since this quantity depends exclusively on the solute-solvent molecular asymmetries (the sources of nonidealities), and thus, it measures directly the solvation strength.

ACKNOWLEDGMENTS

This research was sponsored by the Division of Chemical Sciences, Geosciences, and Biosciences, Office of Basic Energy Sciences, and by the Environmental Management Science Program (TTP OR17-SP22), under Contract No. DE-AC05-00OR22725 with Oak Ridge National Laboratory, managed and operated by UT-Battelle, LLC. P.T.C. was supported by the Division of Chemical Sciences, Geosciences, and Biosciences, Office of Basic Energy Sciences, U.S. Department of Energy. P.G.K. acknowledges the financial support of the Natural Sciences and Engineering Research Council of Canada.

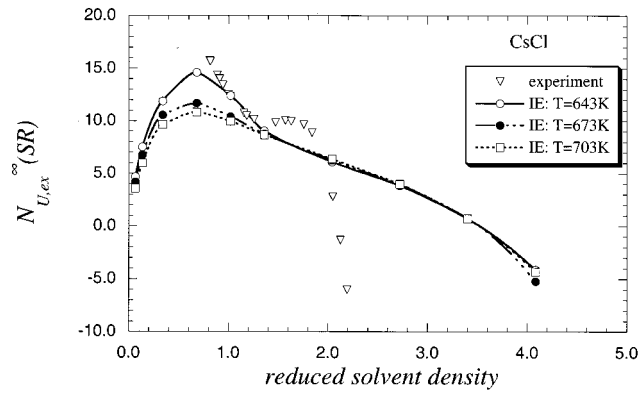

FIG. 17. Density dependence of $N^{\infty}_{U,\mathrm{ex}}(\mathrm{SR})$ for CsCl aqueous solutions. Comparison between RHNC calculations and experimental data.

TABLE III. Coefficients for Eq. (A1).

	$10^2 a_o$(m^3/kg)	$10^4 a_1$	$10^7 a_2$	$10^{10} a_3$
CsBr	−28.721	14.962	−28.467	18.576
NaBr	−27.747	14.405	−27.386	17.784
NaCl	−33.206	18.274	−36.306	24.451

APPENDIX

The regression proposed by Wood and co-workers for D^{∞}_{UV} reads,

$$D^{\infty}_{UV} = a_o + a_1\rho + a_2\rho^2 + a_3\rho^3, \tag{A1}$$

where ρ is the density of pure water in units of kg/m^3, and the coefficients are given in Table III for the three salts of interest.

Based on these values the expression for the CsCl becomes

$$D^{\infty}_{UV} = -0.3418 + 1.8831\times 10^{-3}\rho - 3.7387\times 10^{-6}\rho^2 + 2.5243\times 10^{-9}\rho^3.$$

[1] C. Jeanthon, Antoine van Leeuwenhoek International Journal of General and Molecular Microbiology **77**, 117 (2000).
[2] F. Canganella, A. Gambacorta, C. Kato, and K. Horikoshi, Microbiol. Res. **154**, 297 (2000).
[3] H. Schmieder, J. Abeln, N. Boukis, *et al.*, J. Supercrit. Fluids **17**, 145 (2000).
[4] O. Weiss, G. Ihlein, and F. Schuth, Microporous Mater. **35-6**, 617 (2000).
[5] Y. Kim and D. P. Jung, Inorg. Chem. **39**, 1470 (2000).
[6] Z. B. Wu, T. Tsukada, and M. Yoshimura, J. Mater. Sci. **35**, 2833 (2000).
[7] J. H. Johnston, C. B. Milestone, P. T. Northcote, and N. Wiseman, App. J. **53**, 54 (2000).
[8] A. Shanableh, Water Res. **34**, 945 (2000).
[9] D. B. Mitton, J. C. Orzalli, and R. M. Latanision, in *Physical Chemistry of Aqueous Systems: Meeting the Needs of Industry*, edited by H. J. White, J. V. Sengers, D. B. Neumann, and J. C. Bellows (Begell House, New York, 1995), pp. 638–643.
[10] H. E. Barner, C. Y. Huang, T. Johnson *et al.*, J. Hazardous Mater. **31**, 1 (1992).
[11] M. Modell, in *Standard Handbook of Hazardous Waste Treatment and Disposal*, edited by H. M. Freeman (McGraw–Hill, New York, 1989).
[12] L. A. Torry, R. Kaminsky, M. T. Klein, and M. R. Klotz, J. Supercrit. Fluids **5**, 163 (1992).
[13] A. A. Chialvo and P. T. Cummings, in *Advances in Chemical Physics*, Vol. 109, edited by S. A. Rice (Wiley, New York, 1999), Vol. 109, pp. 115–205.
[14] *Geochemistry of Hydrothermal Ore Deposits*, edited by H. L. Barnes (Wiley, New York, 1997).
[15] R. E. Mesmer, D. A. Palmer, and J. M. Simonson, in *Activity Coefficients in Electrolyte Solutions*, 2nd ed., edited by K. S. Pitzer (CRC Press, Boca Raton, 1991), pp. 491–529.
[16] A. A. Chialvo, P. G. Kusalik, Y. V. Kalyuzhnyi, and P. T. Cummings, J. Stat. Phys. **100**, 167 (2000).
[17] A. A. Chialvo, J. Chem. Phys. **92**, 673 (1990).
[18] J. R. Quint and R. H. Wood, J. Phys. Chem. **89**, 380 (1985).
[19] R. H. Wood, R. W. Carter, J. R. Quint *et al.*, J. Chem. Thermodyn. **26**, 225 (1994).
[20] B. E. Conway, *Ionic Hydration in Chemistry and Biophysics* (Elsevier, Amsterdam, 1981).
[21] A. A. Chialvo and P. T. Cummings, AIChE J. **40**, 1558 (1994).
[22] A. A. Chialvo and P. T. Cummings, Mol. Phys. **84**, 41 (1995).
[23] A. A. Chialvo, P. T. Cummings, J. M. Simonson, and R. E. Mesmer, J. Chem. Phys. **110**, 1064 (1999).
[24] A. A. Chialvo, P. T. Cummings, J. M. Simonson, and R. E. Mesmer, J. Chem. Phys. **110**, 1075 (1999).
[25] J. Sedlbauer, E. M. Yezdimer, and R. H. Wood, J. Chem. Thermodyn. **30**, 3 (1998).
[26] M. S. Gruszkiewicz and R. H. Wood, J. Phys. Chem. B **101**, 6549 (1997).
[27] A. A. Chialvo, Fluid Phase Equilibria **83**, 23 (1993).
[28] A. A. Chialvo, P. G. Kusalik, P. T. Cummings, and J. M. Simonson, J. Phys.: Condens. Matter **12**, 3585 (2000).
[29] P. G. Kusalik and G. N. Patey, J. Chem. Phys. **86**, 5110 (1987).
[30] J. P. O'Connell, in *Fluctuation Theory of Mixtures*, edited by E. Matteoli and G. A. Mansoori (Taylor and Francis, New York, 1990), Vol. 2, pp. 45–67.
[31] J. M. H. Levelt Sengers, in *Supercritical Fluid Technology*, edited by T. J. Bruno and J. F. Ely (CRC Press, Boca Raton, 1991a), pp. 1–56.
[32] A. V. Plyasunov, J. P. O'Connell, R. H. Wood, and E. L. Shock, Geochim. Cosmochim. Acta **64**, 2779 (2000).
[33] J. Seldbauer, J. P. O'Connell, and R. H. Wood, Chem. Geol. **163**, 43 (2000).
[34] J. P. O'Connell, A. V. Sharygin, and R. H. Wood, Ind. Eng. Chem. Res. **35**, 2808 (1996).
[35] J. G. Kirkwood and F. P. Buff, J. Chem. Phys. **19**, 774 (1951).
[36] P. G. Kusalik and G. N. Patey, J. Chem. Phys. **88**, 7715 (1988).
[37] P. G. Kusalik and G. N. Patey, J. Chem. Phys. **89**, 7478 (1988).
[38] P. G. Kusalik and G. N. Patey, J. Chem. Phys. **89**, 5843 (1988).
[39] P. G. Kusalik and G. N. Patey, Mol. Phys. **65**, 1105 (1988).
[40] P. G. Debenedetti and R. S. Mohamed, J. Chem. Phys. **90**, 4528 (1989).
[41] J. M. H. Levelt Sengers, J. Supercrit. Fluids **4**, 215 (1991).
[42] R. H. Wood, 5th International Symposium on Hydrothermal Reactions, Gatlinburg, July 20–24 1997 (personal communication).
[43] Note that a misprint in the expression for $N^{\infty}_{U,\mathrm{ex}}$(SR) has been detected in Eq. (19) of Ref. 28, and in Eq. (52) of Ref. 24. In both cases the first term, $(1-n)$, should be deleted.
[44] Y. Marcus, *Ion Solvation* (Wiley, Chichester, 1985).
[45] M. Magini, G. Licheri, G. Paschina *et al.*, *X-Ray Diffraction of Ions in Aqueous Solutions: Hydration and Complex Formation* (CRC Press, Boca Raton, 1988).
[46] H. Ohtaki and T. Radnai, Chem. Rev. **93**, 1157 (1993).